EuroIntervention 2016;12:1481-1489

Quantification and characterisation of released plaque material during bioresorbable vascular scaffold implantation into right coronary artery lesions by multimodality intracoronary imaging

Heike A. Hildebrandt[1,2]*, MD; Polykarpos C. Patsalis[2], MD; Fadi Al-Rashid[2], MD; Markus Neuhäuser[3,4], PhD; Tienush Rassaf[2], MD; Gerd Heusch[1], MD, PhD; Philipp Kahlert[2], MD; Petra Kleinbongard[1], PhD

1. Institute for Pathophysiology, West German Heart and Vascular Center Essen, University of Essen Medical School, University Duisburg-Essen, Essen, Germany; 2. Department of Cardiology and Vascular Medicine, West-German Heart and Vascular Center Essen, University of Essen Medical School, University Duisburg-Essen, Essen, Germany; 3. Institute for Medical Informatics, Biometry and Epidemiology, University of Essen Medical School, University Duisburg-Essen, Essen, Germany; 4. Department of Mathematics and Technology, Koblenz University of Applied Science, Remagen, Germany

P. Kahlert and P. Kleinbongard contributed equally to this work.

KEYWORDS

- near-infrared spectroscopy
- optical coherence tomography
- periprocedural embolisation
- thin-cap fibroatheroma
- virtual histology intravascular ultrasound

Abstract

Aims: We aimed to compare intravascular ultrasound with virtual histology (VH-IVUS), optical coherence tomography (OCT) and near-infrared spectroscopy (NIRS) for their ability to quantify the true amount and characterise the nature of released plaque material during bioresorbable vascular scaffold (BVS) implantation into right coronary artery (RCA) lesions using a distal occlusion and aspiration device.

Methods and results: Seventeen patients underwent BVS implantation into the right coronary artery under distal protection with intracoronary imaging using VH-IVUS, OCT and NIRS. The amount of released plaque material and its lipid content (LC) were determined. Necrotic core volume and minimal fibrous cap thickness correlated with the amount of released plaque material ($r=0.80$ and $r=-0.65$, respectively) and its LC ($r=0.75$ and $r=-0.78$, respectively), but not maximal lipid core burden index (LCBI). OCT-identified thin-cap fibroatheromata (TCFA) were associated with the greatest amount of released plaque material compared to non-TCFA (46.8 [29.0;49.2] mg vs. 14.2 [11.3;19.4] mg; $p=0.003$) and LC (4.4 [4.0;4.8] mg vs. 2.0 [1.8;2.5] mg; $p=0.000$).

Conclusions: VH-IVUS and OCT but not NIRS parameters quantify and characterise the amount of released plaque material. TCFA is associated with the highest amount of released plaque material and may therefore benefit from the use of protection devices.

**Corresponding author: Department of Cardiology and Vascular Medicine, West German Heart and Vascular Center Essen, University of Essen Medical School, University Duisburg-Essen, Hufelandstr. 55, 45122 Essen, Germany. E-mail: heike.hildebrandt@uk-essen.de*

SUBMITTED ON 07/09/2015 - REVISION RECEIVED ON 1st 30/12/2015 / 2nd 29/04/2016 - ACCEPTED ON 01/06/2016

DOI: 10.4244/EIJ-D-15-00207

Abbreviations

a.u.	arbitrary unit
BVS	bioresorbable vascular scaffold
CAD	coronary artery disease
LC	lipid content
LCBI	lipid core burden index
$LCBI_{lesion}$	lipid core burden index of the lesion
$maxLCBI_{4mm}$	maximal lipid core burden index over any 4 mm segment within the lesion
MI	myocardial infarction
NIRS	near-infrared spectroscopy
OCT	optical coherence tomography
PCI	percutaneous coronary intervention
RCA	right coronary artery
TCFA	thin-cap fibroatheroma
VH-IVUS	intravascular ultrasound with virtual histology

Introduction

Lumen gain by percutaneous coronary intervention (PCI) is achieved by stretching of the vessel with the culprit lesion, dissection, plaque redistribution and embolisation of plaque debris. Microembolisation can induce periprocedural myocardial infarction (MI) in 2-50% of cases[1]. The incidence of periprocedural MI varies depending on the culprit lesion, the type of intervention and the biomarkers/parameters used for its diagnosis[2]. The clinical consequences of periprocedural microembolisation of plaque debris and soluble thrombogenic, vasomotor and inflammatory substances, which contribute to microvascular obstruction[3-5], range from asymptomatic increases in cardiac biomarkers to severe, life-threatening situations. The prognostic relevance of periprocedural MI is still controversial[6]; however, there is consensus to limit myocardial injury as much as possible.

Intracoronary imaging modalities provide insight into the vascular wall and identify certain plaque phenotypes which are particularly susceptible to distal embolisation[7]: intravascular ultrasound with virtual histology (VH-IVUS) can quantify the necrotic core[8,9], optical coherence tomography (OCT) can detect lesions with a thin fibrous cap (thin-cap fibroatheroma [TCFA])[10], and near-infrared spectroscopy (NIRS) quantifies the lesion's maximal lipid core burden[11-13]. These imaging modalities and their distinct parameters have been compared to each other[14-16] and correlated with post-interventional increases of cardiac biomarkers[8,10,17,18]. So far, these imaging parameters have neither been correlated with the true amount of *in vivo* released plaque material nor analysed for their potential to characterise the nature of the embolised material. An imaging parameter, which accurately quantifies the amount and characterises the nature of released plaque material, might allow better prediction of clinical events.

The efficacy of embolisation protection devices during PCI continues to be the subject of controversy, especially in native vessel PCI[19], although their use in saphenous vein grafts is supported by strong evidence and recommended in current guidelines. Apart from a potentially beneficial effect, embolic protection devices offer the opportunity to capture iatrogenically released plaque material, which otherwise embolises into the downstream coronary microcirculation[3]; obviously, with the capture of the released plaque material, the lesion phenotype can no longer be correlated to biomarker release or clinical endpoints. Implantation of bioresorbable vascular scaffolds (BVS) in particular has been associated with a higher incidence of periprocedural MI by increased periprocedural plaque embolisation or side branch occlusion due to a higher strut width and thickness, compared to metal stents[20]. Here, we aimed to compare VH-IVUS, OCT and NIRS for their ability to quantify the true amount and characterise the nature of released plaque material during BVS implantation into right coronary artery (RCA) lesions using a distal occlusion and aspiration device.

Methods

The study was approved by the institutional review board (No. 07-3387) and conducted in accordance with the ethical guidelines of the Declaration of Helsinki 1975. Patients gave written informed consent prior to their inclusion in the study. Twenty patients with stable CAD underwent BVS implantation (Absorb™; Abbott Vascular, Santa Clara, CA, USA) without predilatation into the RCA using an embolic protection device (GuardWire®; Medtronic, Minneapolis, MN, USA). Only patients with RCA lesions were enrolled for anatomical reasons, allowing the use of a distal balloon occlusion and aspiration protection device in order to obtain coronary aspirate with its particulate and soluble plaque material. Troponin I increase within 48 hrs was measured in order to verify protection against periprocedural embolisation. Inflammatory parameters, i.e., counts of leukocytes, C-reactive protein, procalcitonin and interleukin 6, were measured before BVS implantation and within 48 hrs. Comparison of baseline values as well as the maximal increase after the procedure was made between TCFA and non-TCFA.

INTRACORONARY IMAGING

VH-IVUS (Volcano Eagle Eye® Platinum RX Digital IVUS Catheter; Volcano Corporation, San Diego, CA, USA), OCT (C7 Dragonfly™ Imaging Catheter; St. Jude Medical, St. Paul, MN, MA, USA) and NIRS (True Vessel Characterization Imaging System™; Infraredx, Burlington, MA, USA) were performed before and after BVS implantation using standard techniques **(Figure 1A-Figure 1L)**[8,14,17].

Pre-interventional imaging parameters, which have been proposed to predict periprocedural MI, were pre-specified to be correlated with the amount of released plaque material and its lipid content (LC), i.e., necrotic core volume in VH-IVUS[9] **(Figure 1A, Figure 1B)**, minimal fibrous cap thickness in OCT[17] **(Figure 1E, Figure 1F)**, and maximal lipid core burden index over any 4 mm segment within the lesion ($maxLCBI_{4mm}$) in NIRS[11,12] **(Figure 1I, Figure 1J)**. In addition, a dichotomous comparison was performed between OCT-identified TCFA, defined as lesions with a lipid arc >180° and a fibrous cap thickness <65 µm[21], and non-TCFA.

Also, post-interventional imaging parameters were correlated with the amount of released plaque material and its LC. Δ Plaque volume was calculated as the difference between pre- and post-interventional plaque volume in VH-IVUS **(Figure 1B-Figure 1D)**.

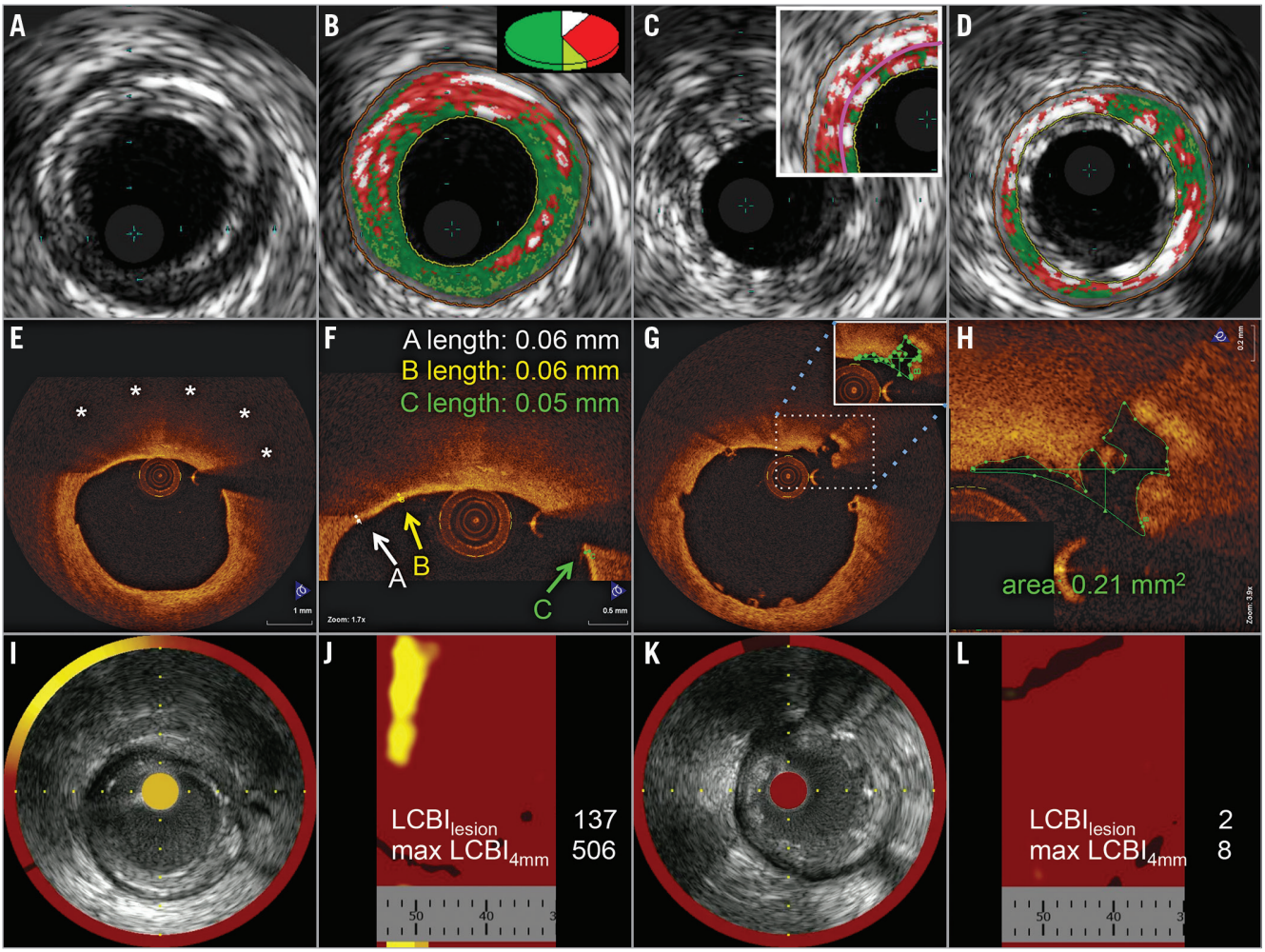

Figure 1. *Pre- and post-interventional VH-IVUS, OCT and NIRS. Corresponding pre-interventional (left two columns) images of VH-IVUS (A-D), OCT (E-H) and NIRS (I-L), showing a TCFA with a large necrotic core (B) in VH-IVUS (dark green: fibrotic, light green: fibro-fatty, red: necrotic core, white: dense calcium), a lipid pool of 180° (E, stars) covered by a thin fibrous cap in OCT (F, arrows) and a high maxLCBI$_{4mm}$ in NIRS (I & J). Post-interventional (right two columns) images show artefacts by BVS struts, misinterpreted as dense calcium by IVUS (C). The plaque volume was determined behind the struts (D), according to Brugaletta et al[30]. OCT shows well-apposed BVS struts and a plaque rupture (G), the circumference of which was manually drawn in every slice (H) over the total length of the treated lesion to allow calculation of the amount of intimal injuries; NIRS shows a reduction of LCBI (K & L).*

In OCT, new endothelial injuries were quantified by volumetry **(Figure 1G, Figure 1H)**. Therefore, in every slice of the BVS-treated lesion, plaque ruptures and dissections were identified, and the area was measured by manually drawing the circumference of each injury. The sum of all measured areas was multiplied by the slice thickness of 0.2 mm, which resulted in a calculated volume. This parameter was termed "volume of intimal injury". In NIRS **(Figure 1I-Figure 1L)**, the difference between the pre- and post-interventional lipid core burden index of the lesion ($\Delta LCBI_{lesion}$) was calculated.

QUANTIFICATION OF RELEASED PLAQUE MATERIAL AND ITS LIPID CONTENT

Coronary aspirate blood was obtained during distal balloon occlusion through an aspiration catheter and directly filtered through a 40 µm mesh filter to separate particulate plaque material. Particulate plaque material was rinsed with NaCl solution (0.9%) in order to clear it from remaining erythrocytes, which would have disturbed our further analysis, i.e., the determination of total lipid content, as erythrocytes contain a high proportion of cholesterols. Released particulate plaque material was weighed and characterised by Pappenheim staining of a smear of residual plaque material, attached to the plastic material of a syringe[22]. Simultaneously to coronary aspiration, venous blood samples were obtained.

LC was determined in particulate plaque material, in coronary aspirate plasma and in venous plasma by lipid extraction, as described by Bligh and Dyer[23]. The amount of released plaque material and its LC were defined as follows: amount of released plaque material=$weight_{particulate\ plaque\ material}$+($LC_{coronary\ aspirate\ plasma}$-$LC_{venous\ plasma}$), LC=$LC_{particulate\ plaque\ material}$+($LC_{coronary\ aspirate\ plasma}$-$LC_{venous\ plasma}$).

Statistical analysis

Image analyses were performed by two independent investigators blinded to the results of the *ex vivo* plaque analyses. The imaging parameters of both investigators were averaged; inter-observer agreement was good (weighted kappa >0.61; data not shown). Since non-normality was shown for some parameters (Shapiro-Wilk test, data not shown), all continuous variables are presented as median (lower quartile; upper quartile) and categorical variables as frequencies (percentages). Spearman's correlations were calculated. Comparison between two groups was performed using the Mann-Whitney U test. Due to the small sample size, exact permutation tests were performed to calculate p-values. All statistics were performed with SPSS software (SPSS Statistics, Version 19.0; IBM Corp., Armonk, NY, USA). A p-value <0.05 was considered significant.

Results

DEMOGRAPHICS AND PROCEDURAL DATA

Patient characteristics and procedural data are presented in **Table 1.** All procedures were performed uneventfully. Asymptomatic peri-interventional troponin I increase to threefold or more above the upper limit of normal within 48 hrs occurred in three cases. Two of these cases had a small, adherent white thrombus in post-interventional OCT, explaining a modest increase of troponin despite the use of a protection device; however, all three cases were excluded from further analysis. There was no significant difference between baseline and maximal increase of inflammatory parameters between TCFA and non-TCFA (data not shown).

In four patients, two BVS were implanted either by one single (n=3) or two separate distal occlusions (n=1). In this case, captured plaque material of both separate occlusions was collected in the same cryotube for further analysis. In one single case, post-interventional OCT revealed partial strut malapposition that required focal post-dilatation, which was not performed under distal occlusion. However, there was no increase in post-interventional troponin in this case. In all cases, post-interventional angiography revealed normal coronary blood flow, filling the distal coronary bed completely; there were no side branch occlusions.

QUANTIFICATION OF THE AMOUNT OF RELEASED PLAQUE MATERIAL AND ITS LIPID CONTENT

The amount of released plaque material was 26.4 (13.1;39.5) mg and its LC was 2.9 (1.9;4.3) mg. Histologic analysis revealed clusters of foam cells surrounded by platelets in all cases **(Figure 2)**.

RELATION BETWEEN IMAGING PARAMETERS AND THE AMOUNT OF RELEASED PLAQUE MATERIAL AND ITS LIPID CONTENT

In VH-IVUS, all lesions consisted of at least three consecutive slides with a necrotic core >10%, OCT identified seven lesions as TCFA and NIRS detected seven lesions with a maxLCBI$_{4mm}$ >500. Interestingly, these lesions did not correspond to each other.

Table 1. Demographics and procedural data.

Demographics		
Age, years		63 (60;70)
Male, n (%)		15 (88)
Height, m		1.71 (1.69;1.75)
Weight, kg		89 (78;95)
Body mass index, kg/m^2		29 (28;30)
Risk factors, n (%)	Hypertension	17 (100)
	Hypercholesterolaemia	17 (100)
	Diabetes mellitus	8 (47)
	Current smoking	4 (24)
	Positive CAD family history	5 (29)
Laboratory	Creatinine, mg/dl	1.16 (1.03;1.31)
	Total cholesterol, mg/dl	168 (155;186)
	Low-density lipoprotein, mg/dl	111 (86;124)
	High-density lipoprotein, mg/dl	39 (36;44)
	Triglycerides, mg/dl	107 (96;166)
	Glycated haemoglobin A1c, %	6.2 (5.6;6.9)
Previous MI, n (%)		4 (24)
Previous coronary artery bypass grafting, n (%)		0 (0)
History of stroke, n (%)		4 (24)
History of peripheral vascular disease, n (%)		2 (12)
Medication, n (%)	Acetylsalicylic acid	17 (100)
	Thienopyridine	17 (100)
	ß-blocker	13 (76)
	Angiotensin-converting enzyme/ angiotensin receptor inhibitor	15 (88)
	Statins	17 (100)
	Antidiabetics	3 (18)
	Diuretics	9 (53)
Procedural data		
RCA segment, n (%)	1	7 (41)
	2	14 (82)
	3	1 (6)
	>1 segment	5 (29)
Quantitative coronary angiography	Diameter stenosis, %	74.7 (70.6;77.3)
	Lesion length, mm	27.5 (17.9;28.0)
Number of BVS implanted/ patient, n (%)	1 scaffold	13 (76)
	2 scaffolds	4 (24)
BVS diameter, mm		3.5 (3.0;3.5)
BVS length, mm		28 (18;28)
Occlusion time, s		165 (150;180)
Fluoroscopy time, min		10 (8;13)
Amount of contrast medium, ml		180 (150;222)

BVS: bioresorbable vascular scaffold; CAD: coronary artery disease; MI: myocardial infarction; RCA: right coronary artery

Pre- and post-interventional imaging parameters and correlations of all analysed imaging parameters are presented in **Table 2** and **Table 3.** In the following paragraphs we focus on the pre-specified imaging parameters.

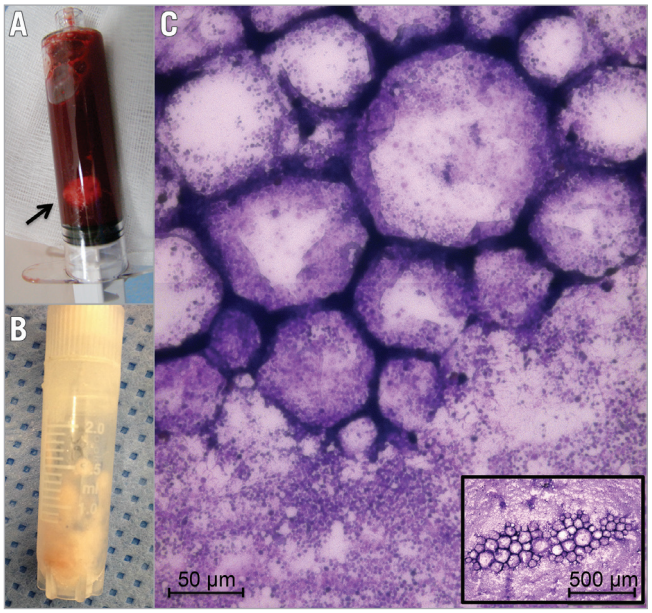

Figure 2. *Released plaque material. Capture of released plaque material, showing a syringe filled with coronary blood and particulate plaque material (A, arrow), a cryotube with separated particulate plaque material, cleared from erythrocytes (B), and a Pappenheim-stained smear, notably clusters of foam cells surrounded by aggregated platelets (C).*

Table 2. Pre- and post-interventional imaging data.

Pre-interventional imaging			
VH-IVUS	Plaque burden, %		63 (59;68)
	Minimal lumen area, mm^2		3.01 (2.64;4.00)
	Plaque volume, mm^3		212.36 (173.60;256.63)
	Media volume, mm^3		66.83 (54.25;85.54)
	Fibrotic tissue	mm^3	88.67 (69.54;104.36)
		%	58.18 (51.32;63.54)
	Fibro-fatty tissue	mm^3	21.59 (13.11;28.90)
		%	15.34 (11.33;17.91)
	Necrotic core	mm^3	28.75 (18.77;45.60)
		%	19.04 (16.27;23.08)
	Dense calcium	mm^3	10.51 (4.13;15.94)
		%	7.51 (4.18;9.94)
OCT	Minimal lumen area, mm^2		2.48 (1.99;2.95)
	Lipid plaque length, mm		13.5 (10.5;18.0)
	Mean lipid arch, °		70.2 (50.5;102.1)
	Maximal lipid arch, °		191.8 (160.5;291.2)
	Lipid index, ° x mm		842.7 (557.3;1,532.1)
	Minimal fibrous cap thickness, mm		0.07 (0.06;0.10)
	TCFA, n (%)		7 (41)
NIRS	$LCBI_{lesion}$ [a.u.]		139 (102;236)
	$maxLCBI_{4mm}$ [a.u.]		436 (222;518)
Post-interventional imaging			
VH-IVUS	Plaque volume, mm^3		170.50 (122.68;209.07)
	Δ Plaque volume, mm^3		50.00 (34.80;64.54)
OCT	Intimal injury, mm^3		2.83 (1.88;3.40)
NIRS	$LCBI_{lesion}$ [a.u.]		48 (23;141)
	$maxLCBI_{4mm}$ [a.u.]		180 (98;299)
	Δ $LCBI_{lesion}$ [a.u.]		67 (22;110)
	Δ $maxLCBI_{4mm}$ [a.u.]		126 (92;297)

a.u.: arbitrary unit; Δ: difference between pre- and post-interventional imaging; $LCBI_{lesion}$: lipid core burden index of the lesion; $maxLCBI_{4mm}$: maximal lipid core burden index over any 4 mm segment within the lesion; NIRS: near-infrared spectroscopy; OCT: optical coherence tomography; TCFA: thin-cap fibroatheroma; VH-IVUS: intravascular ultrasound with virtual histology

Pre-interventional necrotic core volume correlated with the amount of released plaque material and with its LC **(Figure 3A)**. Minimal fibrous cap thickness correlated inversely with the amount of released plaque material and with its LC **(Figure 3B)**. In contrast, $maxLCBI_{4mm}$ correlated neither with the amount of released plaque material nor with its LC **(Figure 3C)**.

The comparison of OCT-identified TCFA versus non-TCFA **(Figure 4)** revealed a higher amount of released plaque material (46.8 [29.0;49.2] vs. 14.2 [11.3;19.4] mg, p=0.003) and a greater LC (4.4 [4.0;4.8] vs. 2.0 [1.8;2.5] mg, p=0.000) in TCFA than in non-TCFA as well as a greater necrotic core volume (46.8 [42.8;49.2] vs. 19.1 [13.3;26.5] mm^3, p=0.000), while there was no significant difference in $maxLCBI_{4mm}$ (506 [276;624] vs. 367 [201;501] a.u., p=0.364).

Post-interventional VH-IVUS-derived Δ plaque volume correlated with the amount of released plaque material and with its LC. Likewise, the OCT-derived volume of intimal injuries correlated with the amount of released plaque material and with its LC. In contrast, Δ $LCBI_{lesion}$ correlated neither with the amount of released plaque material nor with its LC **(Table 3)**.

Discussion

Our study compared current intracoronary imaging modalities for their potential to quantify the amount and characterise the nature of *in vivo* released plaque material during BVS implantation in patients with stable CAD by *ex vivo* analysis of captured plaque material. The amount of released plaque material is reflected by necrotic core volume in VH-IVUS and by minimal fibrous cap thickness in OCT, but not with NIRS-derived $maxLCBI_{4mm}$.

QUANTIFICATION OF THE AMOUNT OF RELEASED PLAQUE MATERIAL

Clinical studies suggest necrotic core in VH-IVUS, and minimal fibrous cap thickness and TCFA in OCT as predictors for periprocedural MI by correlation with cardiac biomarkers or clinical events[9,10,17]. The present study extends such studies to estimate periprocedural embolisation by correlation of distinct imaging parameters with the true amount of *in vivo* released plaque material. The OCT-identified TCFA, which is characterised by a high necrotic core volume in VH-IVUS, is associated with a greater amount of released plaque material than a non-TCFA.

Table 3. Correlations: intracoronary imaging and *ex vivo* plaque analysis.

		Amount of released plaque material		LC of released plaque material	
		Spearman's coefficient	*p*-value	Spearman's coefficient	*p*-value
VH-IVUS	Plaque volume, mm^3	0.620	0.008	0.873	0.000
	Plaque burden, %	0.538	0.031	0.599	0.014
	Fibrotic tissue, mm^3	0.716	0.001	0.714	0.001
	Fibrotic tissue, %	–0.294	0.252	–0.617	0.008
	Fibro-fatty tissue, mm^3	0.221	0.395	0.652	0.005
	Fibro-fatty tissue, %	–0.529	0.029	–0.015	0.955
	Necrotic core, mm^3	0.804	0.000	0.752	0.001
	Necrotic core, %	0.662	0.004	0.310	0.226
	Dense calcium, mm^3	0.529	0.029	0.764	0.000
	Dense calcium, %	0.404	0.107	0.595	0.012
	Δ Plaque volume, mm^3	0.586	0.013	0.737	0.001
OCT	Lipid plaque length, mm	0.318	0.214	0.509	0.037
	Mean lipid arch, °	0.588	0.013	0.726	0.001
	Max lipid arch, °	0.475	0.054	0.781	0.000
	Lipid index, ° x mm	0.549	0.022	0.685	0.002
	Minimal cap thickness, mm	–0.653	0.005	–0.781	0.000
	Intimal injury, mm^3	0.637	0.006	0.524	0.031
NIRS	$LCBI_{lesion}$ [a.u.]	0.034	0.896	0.077	0.768
	$maxLCBI_{4mm}$ [a.u.]	0.250	0.333	0.277	0.282
	Δ $LCBI_{lesion}$ [a.u.]	0.191	0.462	0.112	0.670
	Δ $maxLCBI_{4mm}$ [a.u.]	0.174	0.504	0.172	0.510

a.u.: arbitrary unit; Δ: difference between pre- and post-interventional imaging; LC: lipid content; $LCBI_{lesion}$: lipid core burden index of the lesion; $maxLCBI_{4mm}$: maximal lipid core burden index over any 4 mm segment within the lesion; VH-IVUS: intravascular ultrasound with virtual histology

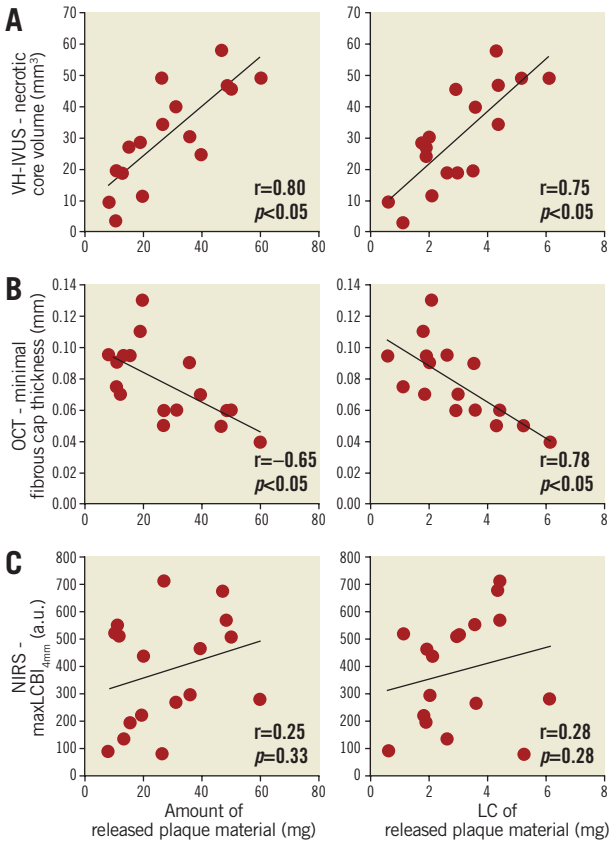

Figure 3. *Quantification and characterisation of released plaque material. Correlations between the amount of released plaque material (left column) and its lipid content (right column) with pre-interventional imaging parameters of VH-IVUS (A), OCT (B) and NIRS (C).*

In contrast to VH-IVUS and OCT, NIRS only shows a tendency to correlate with the amount of released plaque material, although the predominant cells observed in the Pappenheim-stained smear of released plaque material are lipid-rich foam cells, and NIRS has been reported to detect lipids specifically. In line with our observations, the recent large-scale randomised multicentre CANARY trial also did not confirm NIRS parameters as predictors for periprocedural MI or a reduction of periprocedural MI by use of protection devices in lesions presenting with a $maxLCBI_{4mm}$ >600 a.u.[18]. Both the missing correlation to the true amount of released plaque material in our study and the results of the CANARY trial may be explained by the inability of NIRS to determine the depth of a lipid pool[14].

CHARACTERISATION OF THE NATURE OF RELEASED PLAQUE MATERIAL

Until now, imaging parameters have been verified by comparison to pathology specimens[24-27] or indirectly by comparison of different modalities to each other regarding their potential for lipid detection[14-17]. Necrotic core volume (VH-IVUS) is associated with clefts filled with cholesterol and foam cells[28]. TCFA are histologically characterised as lipid-rich plaques covered by only a thin fibrous cap[29], which can be measured by OCT[26]. We here present an association of both VH-IVUS and OCT parameters with the LC of *in vivo* released plaque material.

In addition to the inability of NIRS to quantify the amount of released plaque material, NIRS parameters do not even correlate with its LC. This may be explained by the already mentioned inability to offer a proper axial resolution and a total lipid volume.

POST-INTERVENTIONAL QUANTIFICATION OF THE AMOUNT OF RELEASED PLAQUE MATERIAL AND ITS LC

The difference between pre- and post-interventional imaging parameters is expected to reflect the amount of released plaque material, although this has not been thoroughly validated. In line

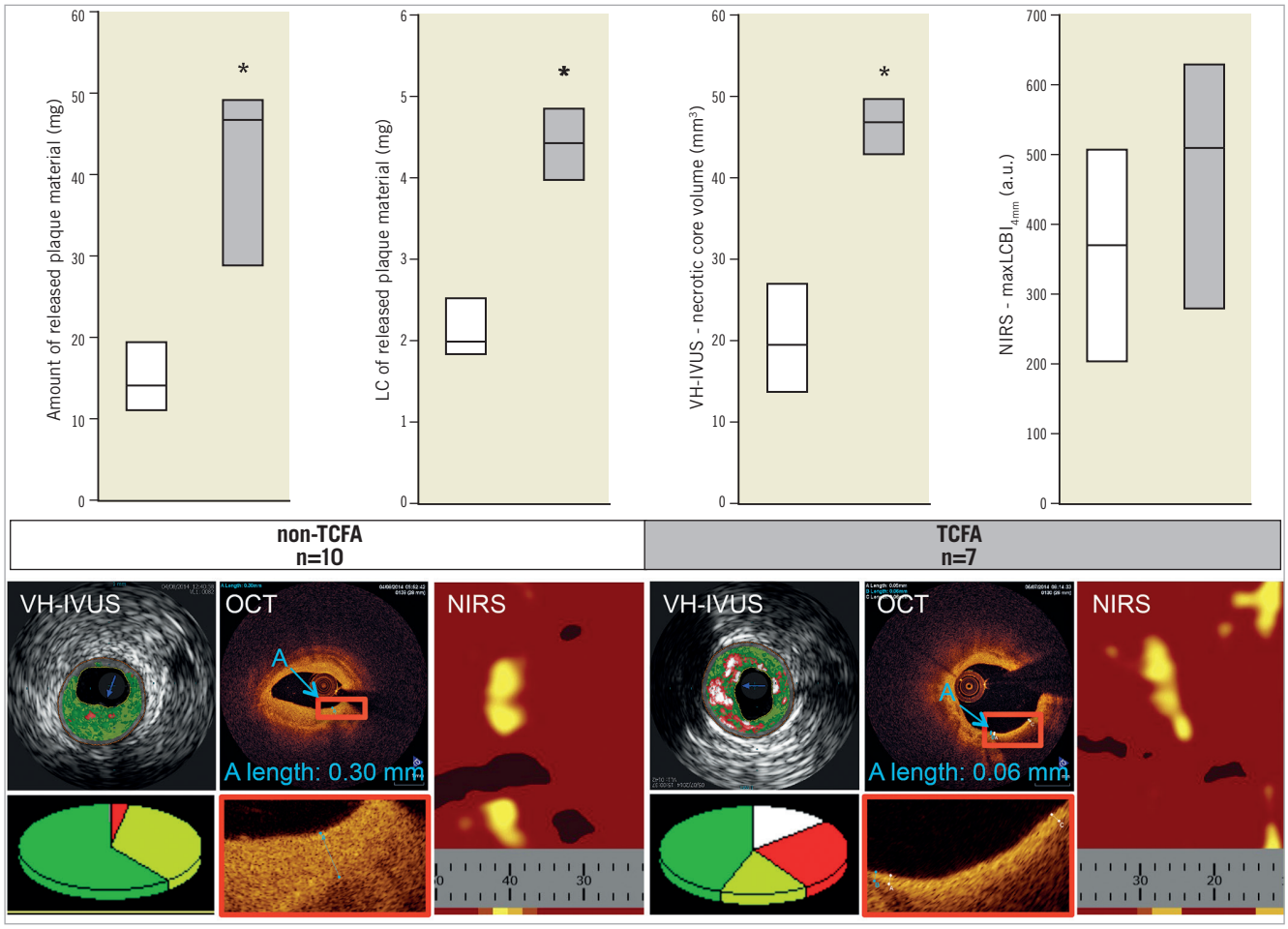

Figure 4. *Comparison between non-TCFA and TCFA. TCFA (grey) are associated with a greater amount and a higher LC of released plaque material than non-TCFA (white). As shown by diagrams and exemplary images of all modalities, TCFA have higher necrotic core volumes than non-TCFA, while there is no significant difference in maxLCBI$_{4mm}$. VH-IVUS - dark green: fibrotic, light green: fibro-fatty, red: necrotic core, white: dense calcium; data are expressed as median (upper quartile; lower quartile). * p<0.05 vs. non-TCFA.*

with this assumption, VH-IVUS-derived Δ plaque volume correlates with the amount of released plaque material and with its LC. Likewise, the OCT-derived volume of intimal injuries correlates with the amount of released plaque material and its LC. Consequently, VH-IVUS and OCT may allow a *post hoc* quantification of released plaque material. Nevertheless, our conclusion is based on correlations between calculated imaging parameters and the amount of released plaque and its LC and is, therefore, only hypothesis-generating.

Since pre-interventional NIRS parameters reflected neither the amount nor the nature of released plaque material, we could not expect and indeed did not determine a correlation with post-interventional Δ LCBI$_{lesion}$. A post-interventional plaque shift and rearrangement of lipid cores from deeper to superficial areas might cause such a lack of correlation. Nevertheless, NIRS revealed an overall reduction of LCBI$_{lesion}$ after BVS implantation. This fact confirms prior studies which reported a PCI-related reduction of LCBI[13,18]. The reduction of LCBI *per se* supports the idea of periprocedural release of lipids, whereas here we demonstrate that this reduction reflects neither the quantity nor the quality of *in vivo* released plaque material.

Limitations

Our study was limited to a small number of patients with stable CAD and RCA lesions; patients with PCI of saphenous vein grafts or with acute MI, who have an even higher risk for periprocedural embolisation, were excluded. The complexity of the procedure with three different imaging catheters performed prior to and after BVS implantation under distal occlusion/protection might have induced a patient selection bias. Clinical endpoints for periprocedural MI, such as increases in troponin I or adverse clinical outcomes, are lacking due to the study's observational nature without randomisation for the use of a protection device.

The selection of patients presenting with stable CAD may be the most important reason to explain why NIRS was incapable of differentiating plaques with a high risk of embolisation from

those without. This fact is in contrast to most published literature. Nevertheless, most studies were performed in patients with acute coronary syndromes who, *per se*, have a higher risk of embolisation. The fact that the CANARY trial enrolled patients with stable angina, silent ischaemia and stabilised acute coronary syndromes might have been an additional factor, explaining the failure of NIRS to predict periprocedural MI in this large-scale, randomised study[18]. Although we observed a post-interventional reduction of LCBI, we could not demonstrate a correlation with the quantity of *in vivo* released plaque material. Of note, artefacts of the BVS struts might have hampered NIRS analysis, which has not been validated so far for lipid detection behind polymeric BVS struts.

Apart from and in addition to the pre-specified necrotic core volume, other VH-IVUS parameters correlated with the amount of released plaque material and its LC **(Table 3)**. This might be explained by the low predictive value of VH-IVUS to distinguish different plaque components.

The OCT-derived quantification of intimal injuries is a new method and must be validated in future studies. Nevertheless, the current results by two independent, blinded investigators were conclusive.

Conclusion

VH-IVUS and OCT but not NIRS parameters can quantify and characterise the amount of *in vivo* released plaque material and its LC in the setting of BVS implantation into RCA lesions for stable CAD. TCFA is associated with the highest amount of plaque material released during BVS implantation, thereby potentially benefiting from the use of protection devices during intervention.

Impact on daily practice

VH-IVUS and OCT but not NIRS parameters can quantify and characterise the amount of released plaque material and its LC, allowing a lesion-specific risk assessment, and thus potentially leading to different treatment algorithms, such as the selective use of protection devices, plaque stabilising medication and/or additional antithrombotic treatment. TCFA appear most vulnerable with the highest amount of plaque material released during BVS implantation, thereby potentially benefiting from the use of protection devices.

Funding

H. Hildebrandt was supported by a research grant from the Medical Faculty of the University Duisburg-Essen (IFORES 10+2).

Conflict of interest statement

The authors have no conflicts of interest to declare.

References

1. Heusch G, Kleinbongard P, Böse D, Levkau B, Haude M, Schulz R, Erbel R. Coronary microembolization: from bedside to bench and back to bedside. *Circulation.* 2009;120:1822-36.

2. Lansky AJ, Stone GW. Periprocedural myocardial infarction: prevalence, prognosis, and prevention. *Circ Cardiovasc Interv.* 2010;3:602-10.

3. Kleinbongard P, Konorza T, Böse D, Baars T, Haude M, Erbel R, Heusch G. Lessons from human coronary aspirate. *J Mol Cell Cardiol.* 2012;52:890-6.

4. Kleinbongard P, Baars T, Möhlenkamp S, Kahlert P, Erbel R, Heusch G. Aspirate from human stented native coronary arteries vs. saphenous vein grafts: more endothelin but less particulate debris. *Am J Physiol Heart Circ Physiol.* 2013;305:H1222-9.

5. Heusch G, Kleinbongard P, Skyschally A. Myocardial infarction and coronary microvascular obstruction: an intimate, but complicated relationship. *Basic Res Cardiol.* 2013;108:380.

6. Prasad A, Herrmann J. Myocardial infarction due to percutaneous coronary intervention. *N Engl J Med.* 2011;364:453-64.

7. Patel VG, Brayton KM, Mintz GS, Maehara A, Banerjee S, Brilakis ES. Intracoronary and noninvasive imaging for prediction of distal embolization and periprocedural myocardial infarction during native coronary artery percutaneous intervention. *Circ Cardiovasc Imaging.* 2013;6:1102-14.

8. Böse D, von Birgelen C, Zhou XY, Schmermund A, Philipp S, Sack S, Konorza T, Möhlenkamp S, Leineweber K, Kleinbongard P, Wijns W, Heusch G, Erbel R. Impact of atherosclerotic plaque composition on coronary microembolization during percutaneous coronary interventions. *Basic Res Cardiol.* 2008;103:587-97.

9. Claessen BE, Maehara A, Fahy M, Xu K, Stone GW, Mintz GS. Plaque composition by intravascular ultrasound and distal embolization after percutaneous coronary intervention. *JACC Cardiovasc Imaging.* 2012;5:S111-8.

10. Lee T, Murai T, Yonetsu T, Suzuki A, Hishikari K, Kanaji Y, Matsuda J, Araki M, Niida T, Isobe M, Kakuta T. Relationship between subclinical cardiac troponin I elevation and culprit lesion characteristics assessed by optical coherence tomography in patients undergoing elective percutaneous coronary intervention. *Circ Cardiovasc Interv.* 2015;8(4).

11. Goldstein JA, Grines C, Fischell T, Virmani R, Rizik D, Muller J, Dixon SR. Coronary embolization following balloon dilation of lipid-core plaques. *JACC Cardiovasc Imaging.* 2009;2:1420-4.

12. Goldstein JA, Maini B, Dixon SR, Brilakis ES, Grines CL, Rizik DG, Powers ER, Steinberg DH, Shunk KA, Weisz G, Moreno PR, Kini A, Sharma SK, Hendricks MJ, Sum ST, Madden SP, Muller JE, Stone GW, Kern MJ. Detection of lipid-core plaques by intracoronary near-infrared spectroscopy identifies high risk of periprocedural myocardial infarction. *Circ Cardiovasc Interv.* 2011;4:429-37.

13. Brilakis ES, Abdel-Karim AR, Papayannis AC, Michael TT, Rangan BV, Johnson JL, Banerjee S. Embolic protection device utilization during stenting of native coronary artery lesions with large lipid core plaques as detected by near-infrared spectroscopy. *Catheter Cardiovasc Interv.* 2012;80:1157-62.

14. Yonetsu T, Suh W, Abtahian F, Kato K, Vergallo R, Kim SJ, Jia H, McNulty I, Lee H, Jang IK. Comparison of near-infrared

spectroscopy and optical coherence tomography for detection of lipid. *Catheter Cardiovasc Interv.* 2014;84:710-7.

15. Roleder T, Kovacic JC, Ali Z, Sharma R, Cristea E, Moreno P, Sharma SK, Narula J, Kini AS. Combined NIRS and IVUS imaging detects vulnerable plaque using a single catheter system: a head-to-head comparison with OCT. *EuroIntervention.* 2014;10:303-11.

16. Pu J, Mintz GS, Brilakis ES, Banerjee S, Abdel-Karim AR, Maini B, Biro S, Lee JB, Stone GW, Weisz G, Maehara A. In vivo characterization of coronary plaques: novel findings from comparing greyscale and virtual histology intravascular ultrasound and near-infrared spectroscopy. *Eur Heart J.* 2012;33:372-83.

17. Kini AS, Motoyama S, Vengrenyuk Y, Feig JE, Pena J, Baber U, Bhat AM, Moreno P, Kovacic JC, Narula J, Sharma SK. Multimodality intravascular imaging to predict periprocedural myocardial infarction during percutaneous coronary intervention. *JACC Cardiovasc Interv.* 2015;8:937-45.

18. Stone GW, Maehara A, Muller JE, Rizik DG, Shunk KA, Ben-Yehuda O, Genereux P, Dressler O, Parvataneni R, Madden S, Shah P, Brilakis ES, Kini AS; CANARY Investigators. Plaque Characterization to inform the Prediction and Prevention of Periprocedural Myocardial Infarction During Percutaneous Coronary Intervention: The CANARY trial (Coronary Assessment by Near-infrared of Atherosclerotic Rupture-prone Yellow). *JACC Cardiovasc Interv.* 2015;8:927-36.

19. Jin B, Dong XH, Zhang C, Li Y, Shi HM. Distal protection devices in primary percutaneous coronary intervention of native coronary artery lesions: a meta-analysis of randomized controlled trials. *Curr Med Res Opin.* 2012;28:871-6.

20. Kawamoto H, Panoulas VF, Sato K, Miyazaki T, Naganuma T, Sticchi A, Figini F, Latib A, Chieffo A, Carlino M, Montorfano M, Colombo A. Impact of Strut Width in Periprocedural Myocardial Infarction: A Propensity-Matched Comparison Between Bioresorbable Scaffolds and the First-Generation Sirolimus-Eluting Stent. *JACC Cardiovasc Interv.* 2015;8:900-9.

21. Lee SY, Hong MK, Shin DH, Kim JS, Kim BK, Ko YG, Choi D, Jang Y. Optical coherence tomography-based predictors for creatine kinase-myocardial band elevation after elective percutaneous coronary intervention for in-stent restenosis. *Catheter Cardiovasc Interv.* 2015;85:564-72.

22. Hildebrandt HA, Kahlert P, Baars T, Kleinbongard P, Erbel R, Heusch G. Is there a need for distal protection during native vessel percutaneous coronary intervention in patients with stable coronary artery disease? *J Cardiovasc Med (Hagerstown).* 2014;15:170-2.

23. Bligh EG, Dyer WJ. A rapid method of total lipid extraction and purification. *Can J Biochem Physiol.* 1959;37:911-7.

24. Nasu K, Tsuchikane E, Katoh O, Vince DG, Virmani R, Surmely JF, Murata A, Takeda Y, Ito T, Ehara M, Matsubara T, Terashima M, Suzuki T. Accuracy of in vivo coronary plaque morphology assessment: a validation study of in vivo virtual histology compared with in vitro histopathology. *J Am Coll Cardiol.* 2006;47:2405-12.

25. Yabushita H, Bouma BE, Houser SL, Aretz HT, Jang IK, Schlendorf KH, Kauffman CR, Shishkov M, Kang DH, Halpern EF, Tearney GJ. Characterization of human atherosclerosis by optical coherence tomography. *Circulation.* 2002;106:1640-5.

26. Kume T, Akasaka T, Kawamoto T, Okura H, Watanabe N, Toyota E, Neishi Y, Sukmawan R, Sadahira Y, Yoshida K. Measurement of the thickness of the fibrous cap by optical coherence tomography. *Am Heart J.* 2006;152:755.e1-4.

27. Gardner CM, Tan H, Hull EL, Lisauskas JB, Sum ST, Meese TM, Jiang C, Madden SP, Caplan JD, Burke AP, Virmani R, Goldstein J, Muller JE. Detection of lipid core coronary plaques in autopsy specimens with a novel catheter-based near-infrared spectroscopy system. *JACC Cardiovasc Imaging.* 2008;1:638-48.

28. Nair A, Kuban BD, Tuzcu EM, Schoenhagen P, Nissen SE, Vince DG. Coronary plaque classification with intravascular ultrasound radiofrequency data analysis. *Circulation.* 2002;106:2200-6.

29. Virmani R, Kolodgie FD, Burke AP, Farb A, Schwartz SM. Lessons from sudden coronary death: a comprehensive morphological classification scheme for atherosclerotic lesions. *Arterioscler Thromb Vasc Biol.* 2000;20:1262-75.

30. Brugaletta S, Garcia-Garcia HM, Garg S, Gomez-Lara J, Diletti R, Onuma Y, van Geuns RJ, McClean D, Dudek D, Thuesen L, Chevalier B, Windecker S, Whitbourn R, Dorange C, Miquel-Hebert K, Sudhir K, Ormiston JA, Serruys PW. Temporal changes of coronary artery plaque located behind the struts of the everolimus eluting bioresorbable vascular scaffold. *Int J Cardiovasc Imaging.* 2011;27:859-66.